

Mental Stress Detection Based on Stereo Vision Fusion Measurement

Mohd Norzali Haji Mohd^{1,*}, Masayuki Kashima², Kiminori Sato², Mutsumi Watanabe²

¹Department Of Computer Engineering, Faculty of Electrical and Electronic Engineering, University Tun Hussein Onn Malaysia (UTHM), Parit Raja, Batu Pahat Johor, Malaysia.

²Department of Information Science and Biomedical Engineering, Graduate School of Science and Engineering , Kagoshima University, Korimoto 1-21-40,Kagoshima, 890 0065,Japan.

*Corresponding email: norzali@uthm.edu.my

Abstract

This paper aims to present a novel methodology for real time monitoring of Internal Emotion State (Mental Stress). The method does not require any contact as contact measurement tend to effect emotions and burden physiologically. We have found out that user stress is correlated with the increased blood flow in three facial areas of sympathetic importance which is periorbital, supraorbital and maxillary. This increased blood flow dissipates convective heat which can be monitored through thermal imaging. In the stress experiment conducted, blood vessel is also detected via thermal imaging for several subjects in real time. Thermal infrared and visible cameras are being used in the stimulus experiment. Sample of several faces are also taken in real time in our experimental setup to measure the effectiveness of our method. Almost 98% of correct measurement of ROI and temperature was detected. The results of temperature before and after stress stimulus experiment are also compared and show promising results.

In this paper also, a new method for detecting facial feature in both thermal and visual is presented by applying Nostril Mask, which allows one to find facial feature namely nose area in thermal and visual. Graph Cut algorithm is applied to remove unwanted ROI and correctly detect precise temperature values. Extraction of thermal-visual facial feature images is done by using Scale Invariant Feature Transform (SIFT) Feature detector and extractor to verify the method of using nostril mask. Based on the experiment conducted, it shows 88.6% of correct matching. The detection result of eyes blinking also show promising results.

An Accurate and efficient thermal-infrared camera calibration is also important for advancing computer vision research approach for geometrically calibrating individual and multiple cameras in both thermal and visible modalities. We also propose new printed Fever Cold Plaster (FCP) chessboard using a popular existing approach which is comparatively accurate and simple to execute. Based on the experiment conducted by comparing the degradation of image quality with the current

approach, our proposed chessboard can be more clearly located than those on the applied standard chessboard by 39%.

Keywords: camera calibration; face and gesture recognition; edge and feature detection; image processing software

1. INTRODUCTION

Various methods for internal state measurement such as mental stress have been previously proposed which utilizes the changes of physiological quantities such as blood pressure, heart rate, salivary amylase and electromyography (EMG) [1]. These quantities can be measured invasively by the use of expensive instruments. In this paper we introduce an integrated non-invasive measurement through purely imaging means. The proposed booth setup is equipped with Thermal IR and Visual Camera Sensors. A monitor and a speaker are also installed to provide mental and acoustic stimulus to monitor changes in facial sign and brain waves. These experiments will be done at a later stage.

Face recognition system based on visual images have reached significant level of maturity with some practical success. However, the performance of visual face recognition may degrade under poor illuminations conditions, for subjects of various skin colour and the changes in facial expression. The use of infrared in face recognition allows the limitations of visible face recognition to be overcome. However, infrared suffers from other limitations like opacity to glasses. The overlap between segmented and ground truth.

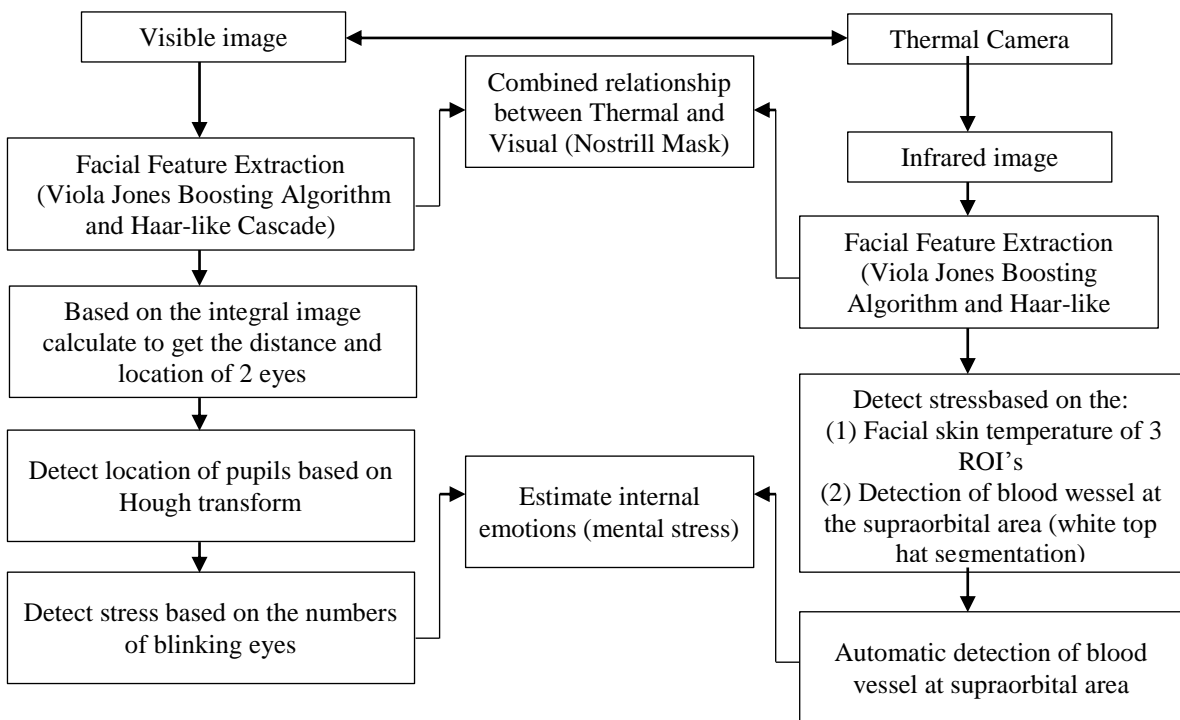


Figure 1: Overall System.

Multi modal fusion comes with the promise of combining the best of each modalities and overcoming their limitations [2]. Facial feature in thermal is difficult to locate because of the poorer contrast between the features and the face in IR images. In

this paper, one common feature that can be automatically located in both thermal-visible domains is the nostril area. This is due to the changes of temperature in nostril area in thermal domain and the higher contrast value in visual domain. An outline of our approach is shown in Figure 1. The combined relationship includes two parts: 1) The relative position between the thermal and visible camera that are calibrated using special calibration board [3]. 2) The relative position and head pose based on nostril mask in thermal and visible. We have also analysed the use of SIFT descriptor as feature matching in thermal and visual domain to verify our method using nostril mask [4]

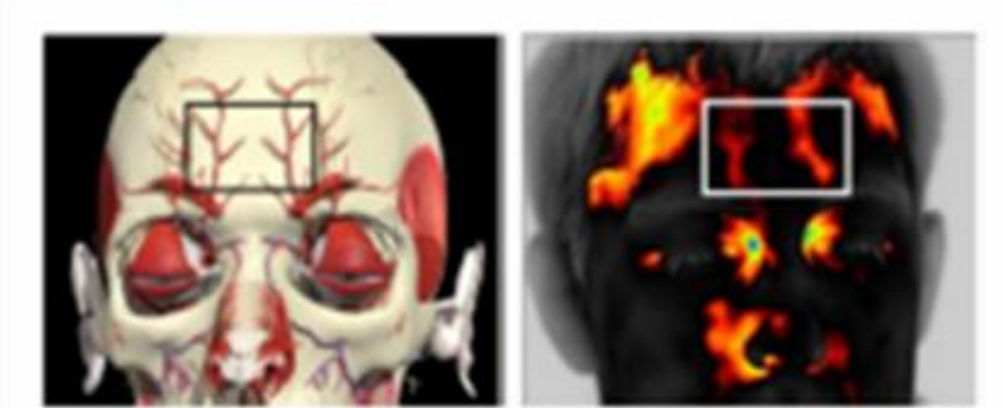


Figure 2: (a) Forehead Anatomy, (b) Thermal facial during stress (MWIR).

This paper presents a novel methodology for real time monitoring of internal emotion state particularly mental stress. The method does not require any contact as con-tact measurement tend to effect emotions and burden physiologically. Based on recent study [5, 6 and 7] con-ducted, we have found out that user stress is correlated with the increased blood flow in three facial areas of sympathetic importance which is periorbital, supraorbital and maxillary. This increased blood flow dissipates convective heat which can be monitored through mid-wave infrared (MWIR, 3-5 μ m) camera (Figure 2 (b)) [8]. Our approach is different which is trying to implement it on a long-wave infrared (LWIR, 8-14 μ m) cam-era.

2. PROPOSED SYSTEM

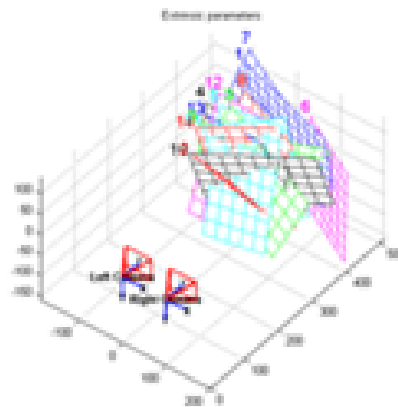
2.1 Image Registration and Collaboration

The relative position between the IR and visible cameras is calibrated by using the special calibration board suggested previously [9]. With some small adjustment and preparation where cold fever plasters are attached to the back of the calibration points on a chessboard, the calibration points can be reliably located in thermal IR and visible domain.

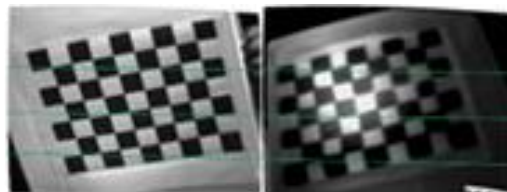
One of the common strategies to simplify correspondence problem between IR and visible domain is to exploit epipolar geometry (Figure 3 (b)). The relative position between thermal-visible stereo cameras is calculated using the heated calibration board which is due to the emissivity difference between the black and white squares on the grid. The output of the calibration method includes the relative rotation and translation of the cameras as well as the internal parameters.



(a)



(b)



(c)

Figure 3: (a) Calibration board (b) Initial calibration and fusion of the IR and visible-spectrum sensors. (c) Computing fundamental matrix and drawing epipolar lines from Thermal-Visual stereo calibrated images.

2.2 Image Calibration of Thermal IR and Visible Stereo Camera

The output of the calibration method includes the relative rotation R and translation T of the cameras with respect to the left hand view and the internal parameters of each camera, focal length f_c , principal point c_c , skew coefficients α_c and radial and

tangential distortion k_c . Following stereo calibration, coordinates of a 3D point, $p_c = [x_c, y_c, z_c]$ as follows $P_c = T + RP$, where R and T are their respective relative rotation and translation with respect to the world coordinates. Here, for the surface reconstruction procedure, we make use of the image point projection of the scene normalized so as to follow the pinhole camera model [10], Let the normalized (pinhole) image projection, $p_n = [x, y]$ be given by:

$$p_n = \begin{bmatrix} x_c/y_c \\ y_c/y_c \end{bmatrix} = \begin{bmatrix} x \\ y \end{bmatrix}. \quad (1)$$

After including the lens distortions, the new normalized point coordinates $p_d = [x_d, y_d]$ is obtained

$$p_d = \begin{bmatrix} x_d \\ y_d \end{bmatrix} = (1 + kc(1)r^2 + kc(2)r^4 + kc(5)r^6)p_n + dx \quad (2)$$

Where $r^2 = x^2 + y^2$, and dx is the tangential distortion vector

$$dx = \begin{bmatrix} 2kc(3)x + kc(4)(r^2 + 2x^2) \\ kc(3)(r^2 + 2y^2) + 2kc(4)xy \end{bmatrix}$$

With these ingredients, we can relate the normalized coordinate vector, p_d , and the pixel image coordinates, x_d and y_d as follows

$$\begin{bmatrix} x_p \\ y_p \\ 1 \end{bmatrix} = K \begin{bmatrix} x_d \\ y_d \\ 1 \end{bmatrix} \quad (3)$$

Where K is known as the camera parameter matrix, which can be expressed making use of the calibration output variables as

$$K = \begin{bmatrix} f_c(1) & \alpha_c * f_c(1) & cc(1) \\ 0 & f_c(2) & cc(2) \\ 0 & 0 & 1 \end{bmatrix}$$

2.3 Final Facial Feature Extraction for Thermal Domain

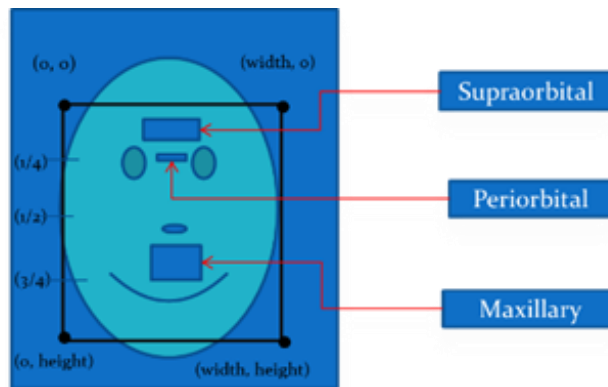


Figure 4: ROI with sympathetic importance.

Thermal face image analysis has many applications such as sensation evaluation and face recognition. Facial feature extraction in the IR image is an essential step in these applications. Certain facial areas such as periorcular, nasal, cheeks and neck region produce different thermal patterns for different activities or emotions[11]. Skin temperature of facial features, such as the nose and forehead, could be an effective

indicator in objectively evaluating human sensations such as stress and fatigue [12][13]. Most existing approaches manually locate the facial feature in IR image or the subject are required to wear marker[14], as it is hard to automatically locate facial features, even for the obvious features such as the corners of the eyes and mouth. This problem is caused by poorer contrast between the features and the face in IR images.

In our experiment, we have found out that by using the proposed face detection using Cascade structure with Haar-like in both Thermal and Visual can detect faces automatically. Measurement is done at three facial areas of sympathetic importance which is periorbital, supraorbital and maxillary (Fig. 4). Based on the past researches [15],[16] and [17], we have found out that 3 ROIs are the most affected during Mental Stress and focuses on the temperature in these areas.

In our experiment, at first, we detect the face region using Viola and Jones's Boosting algorithm [13] and a set of Cascade structure with Haar-like features. Then 3 ROIs are detected based on detected face ratio. The collaboration of ROI with temperature value was done based on the relationship as in [4].

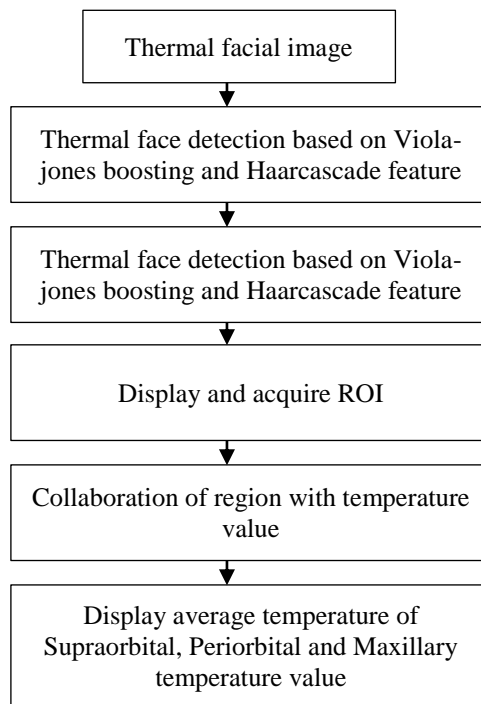


Figure 5: Flowchart of face detection and temperature acquisition in thermal domain.

This relationship is concluded through several experiments done to ensure the accuracy. The average brightness value located around these 3 main areas is then converted to the temperature value.

$$\text{Temperature} = 0.0819 * \text{GrayLevel} + 23.762 \quad [4]$$

Next, we assume that the centroid of the detected face area as nose area and nostril mask is used to recalculate the detected area and map into the facial thermal image (Figure 6).

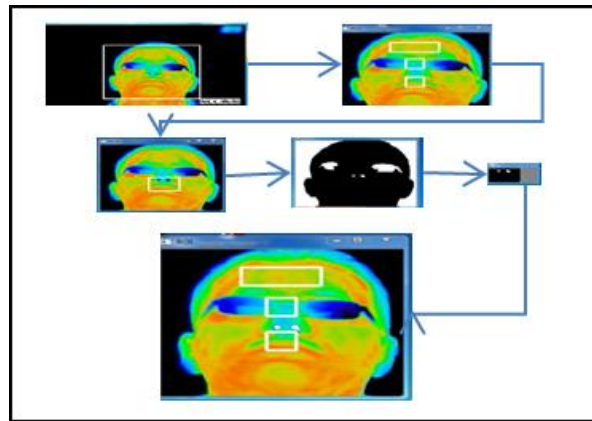


Figure 6: Proposed Automatic Thermal Face, Supraorbital, Periorbital, Maxillary and Nostril Detection.

We then analyze the detected thermal face with the 3 ROIs with sympathetic importance for person wearing spectacles and without it. We found out that there are unwanted ROI such as spectacles and hair which can be excluded so that temperature reading can be done precisely (Figure 7). To overcome this problem, unwanted ROI is removed by using Graph Cut method [12]. We have concluded that the average differences before and after cropping is about 0.3-0.6 °C (Figure 8).

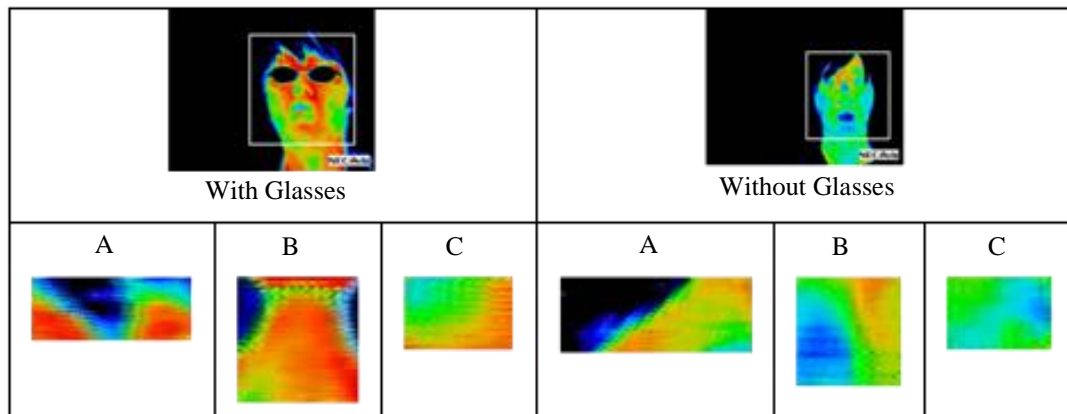


Figure 7: Detected thermal face with and without spectacles

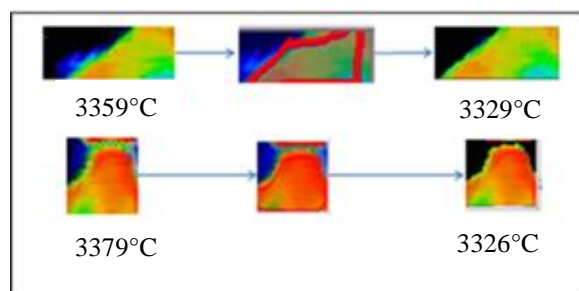


Figure 8: The unwanted ROI removed using Graph Cut

One of the most salient manifestation of sustained stress is that eyebrows frown frequently [18],[19].The frowning is caused by contraction of the corrugator muscle. Activation of the corrugator muscle requires more blood, which is drawn from supraorbital vessels. Increased of the blood flow in the supraorbital vessels, directly increase the cutaneous temperature on the forehead. Our task is to detect elevated stress levels through quantification of increased vessel temperature in thermal imagery.

The proposed methodology for detecting blood vessel as in the flow chart below, (Figure 9 (a)) . After the detection of supraorbital area in thermal IR , image morphology is applied on the diffused image to extract the blood vessels that are relatively low contrast compared with the surrounding tissue. We employ, top-hat segmentation method, which is the combination of the erosion and dilation operations. We are interested in the bright (hot) like structure which correspond to Blood Vessel. For this reason we employ White Top-Hat segmentation (WTH) as in equations [5].

$$I \circ S = (I \ominus S) \oplus S \quad [4] \quad , \quad WTH = I - (I \circ S) \quad [5]$$

Where I : Original Image, $I \circ S$: Opened Image, $I \bullet S$:Closed Image , S :Structuring element, \ominus : Erosion, \oplus :Dilation.

In order to enhance the edge and reduce noise bilateral filter is the employed. Bilateral filter is a nonlinear, edge preserving and noise reducing smoothing filter. The intensity value at each pixel in an image is replaced by a weighted average of intensity values from nearby pixels.

$$I^{filtered}(x) = \sum_{x_i \in \Omega} I(x_i) f_r(\|I(x_i) - I(x)\|) g_s(\|x_i - x\|) \quad [6]$$

where: $I^{filtered}$ is the filtered image; I is the original input image to be filtered; x is the coordinates of the current pixel to be filtered; Ω is the window centered in x ; f_r is the range kernel for smoothing differences in intensities.

This function can be a Gaussian function; g_s is the spatial kernel for smoothing differences in coordinates.

After applying bilateral filter, based on the RGB pixel value, the red range of pixel which is associated to blood vessel is then segmented (Figure 9 (b)) .

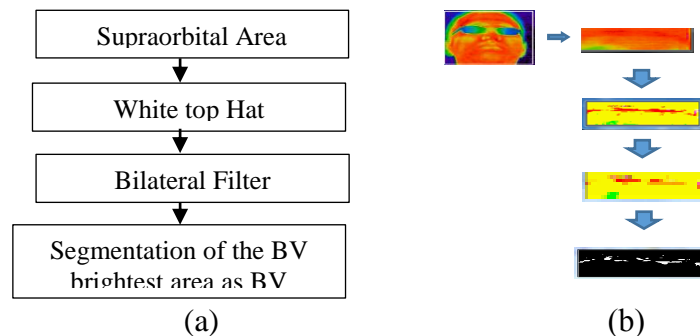


Figure 9: Blood Vessel (BV) at supraorbital Recognition System

2.4. Final Facial Feature Extraction for Visual Domain

The same approach for locating face image in visual face is also done. At first we detect the face using Viola and Jones' Boosting algorithm and a set of Cascade structure with Haar-like features. Next, we assume that the centroid of the detected face area as nose area and nostril mask is used to recalculate the detected area and map into the facial image (Figure10).

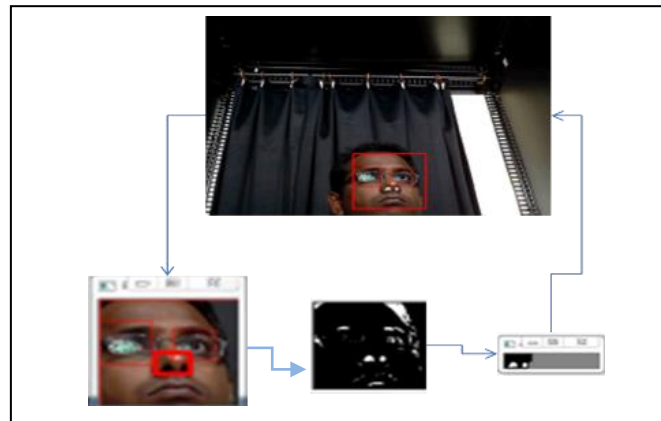


Figure 10: Proposed Automatic Facial and Nostril Detection.

Figure 11, below shows the propose blinking recognition system. After the detection of face based on cascade structure with Haar-like features, the eye part is located by calculating the edge of the eyes which is considered as the brightest part of the face . Next Integral Image is calculated to determine the exact location of eyes and iris. Then based on the pixel value of iris masking, blinking is determined.

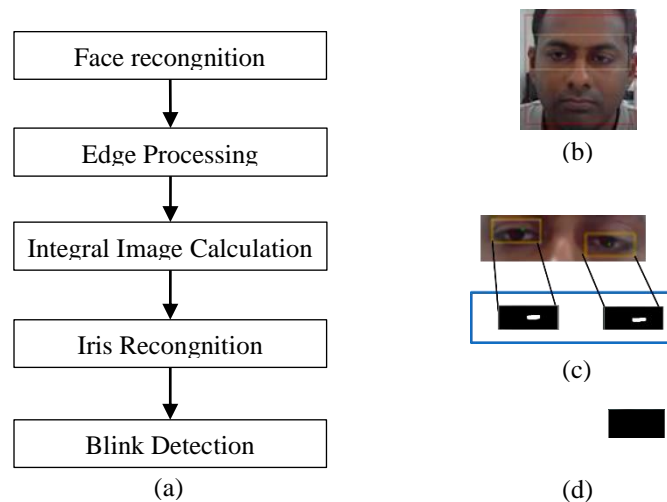


Figure 11: (a) Blinking Recognition System Flow ,(b) Face Recognition based on Cascade structure with Haar-like features, (c) Iris Masking (Eyes open), (d) Iris Masking (Eyes close state)

3. EXPERIMENTS AND RESULTS

To evaluate the alternative approaches and the effectiveness of the proposed calibration board, MRE (Multiple Regression *Equations*) is used as the metric for comparison. The MRE (Multiple Regression *Equations*)[7] are used as the metric for comparison. In general, it is calculated using only frames included in the calibration process. We choose to calculate MRE using entire input that has not actually been selected for calibration. The units are in pixels.

$$\text{MRE} = \frac{\sum_{m=1}^M \sum_{n=1}^N ||p(m,n) - q(m,n)||}{MN} \quad [7]$$

M , is the total number of frames in the extended sequence, and N is the total number of calibration points per frame. $p(m,n)$ is the pixel location of a point in the pattern, and $q(m,n)$ is the projected location of that point using an estimate of the pose of the pattern in the particular frame.

The experiment is conducted in a normal office environment, with an ambient temperature of approximately 24°C. The calibration objects are placed at the minimum focal distances for which the pattern is fully visible, approximately 50cm from the lens. A workspace approximately 1m³ is required for the experiment.

The proposed calibration board is evaluated and compared with existing approaches for calibrating thermal and visual cameras. 100 calibration frames of each pattern are used to compare performance. 2 types of chessboard are printed on an A4 sheet paper. One type which is the conventional chessboard and another is the fever plaster which is in the cool gel form is attached at the back of the chessboard as in figure 2(A). A 500 W heat lamp is used for approximately 5s to heat the pattern as even as possible. Footage is then captured immediately for approximately 10s, at which point the image contrast had degenerated significantly. An identical software framework is used for both method. OpenCV function “findChessboardCorners()” is used.

Table 1: Pattern Effectiveness (MRE And Standard Deviation).

Configuration	MRE
Thermal (chessboard)	0.814±0.015px
Thermal (<i>FCP</i>)	0.614±0.011px

From the above table, it is clear that calibration points on the proposed chessboard *FCP* can be more clearly located than those on the standard chessboard.

Table 2: Intrinsic Parameters of the Two Cameras.

Camera	Thermal Camera (right)	Visual camera(left)
Matrix	$\begin{bmatrix} 270.02 & 0 \\ 0 & 240.15 \\ 0 & 0 \end{bmatrix}$	$\begin{bmatrix} 272.34 & 0 \\ 0 & 268.15 \\ 0 & 0 \end{bmatrix}$
Optical Distortions coefficient s	K1: -0.39235 K2: 0.25438 P1: 0.0011792 P2: 0.0051091	K1: -0.42242 K2: 1.1506 P1: -0.001509 P2: 0.0004468

Table 3: Extrinsic Parameters of the Two Cameras Relating to its Position.

	Visual vs. Thermal
Rotation Matrix	$\begin{bmatrix} 0.999938 & 0.018628 \\ -0. & 315.41 \\ -0.029975 & 0 \end{bmatrix}$
Translation Vector	$\begin{pmatrix} -79.829 \\ -0.92904 \\ -0.023286 \end{pmatrix}$

In the experiment conducted, Scale Invariant Feature Transform (SIFT) is employed to extract facial features in both thermal and visual and to verify our algorithm. SIFT features are features extracted from images to help in reliable matching between different views of the same object [12]. The extracted features are invariant to scale and orientation, and are highly distinctive of the image. They are extracted in four steps. The first step computes the locations of potential interest points in the image by detecting the maxima and minima of a set of Difference of Gaussian (DoG) filters applied at different scales all over the image. Then, these locations are refined by discarding points of low contrast. An orientation is then assigned to each key point based on local image features. Finally, a local feature descriptor is computed at each key point. This descriptor is based on the local image gradient, transformed according to the orientation of the key point to provide orientation invariance. Every feature is a vector of dimension 128 distinctively identifying the neighborhood around the key point.

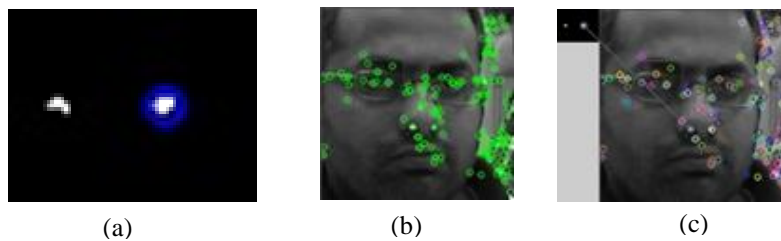


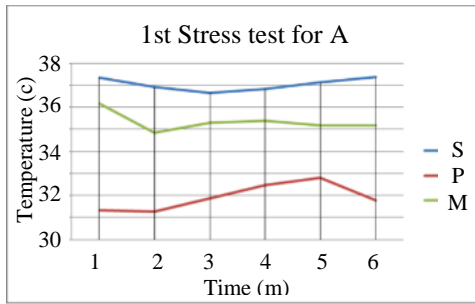
Figure 12: (a) Nostril Mask in Thermal, (b) Facial Sift Feature in Visual (c) Sift Feature Matching

At first, the nostril area in thermal IR is detected using our pair calibrated Thermal –Visible camera. Then, the face part in visible domain is detected and SIFT feature point is calculated in both domain (Figure 9). The feature matching is done and recorded as in Table 4.

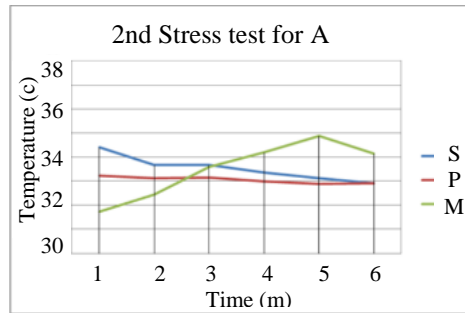
Table 4: Feature Matching Between Nostril Mask (Thermal)- Visible Camera

Frame	Feature Point 1 (TH)	Feature Point 2 (VI)	Processing Time [ms]	Correct Matching
1	2	157	170.759	100
2	2	93	168.443	100
3	11	106	171.866	36
4	2	81	162.892	100
5	2	168	170.921	50
6	1	168	154.105	100
7	1	114	160.873	100
8	1	112	153.269	100
9	1	146	170.35	100
10	1	157	170.972	100

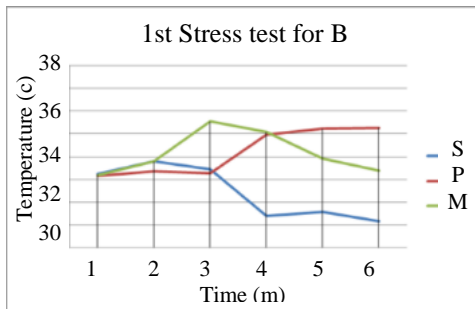
To evaluate our methodology, the experiment is conducted towards 5 subjects, tested for two times of stress stimulus experiment. The reason for conducting two times test to the subjects is to ensure that the subjects are free from any kind of stress. The subjects are also given 1 minute rest to make them calm and neutral. We utilise the stress test which is very well established method for inducing stress. Mental stress experiment, Colour word test is designed by Dr Soren Brage of MRC Epidemiology unit, Cambridge University, which consists of 2 minutes test (120 Slides), 30 seconds rest and 2 minutes test (120 Slides).



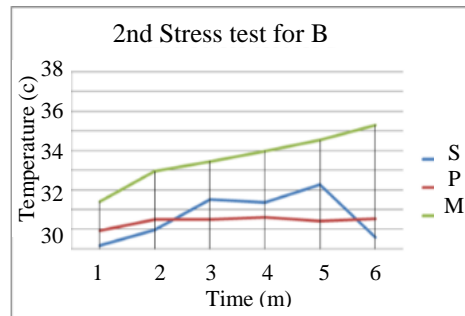
(A2)



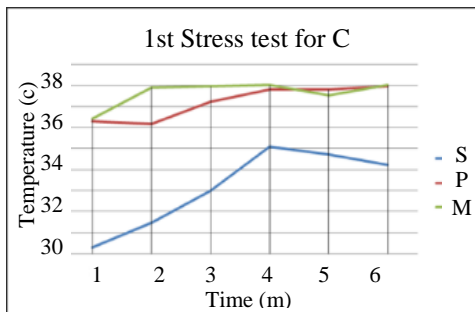
(A1)



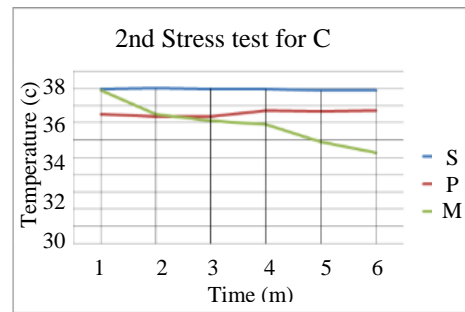
(B2)



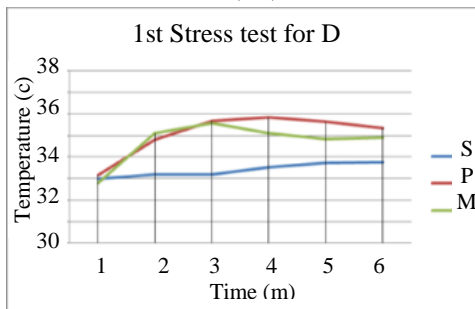
(B1)



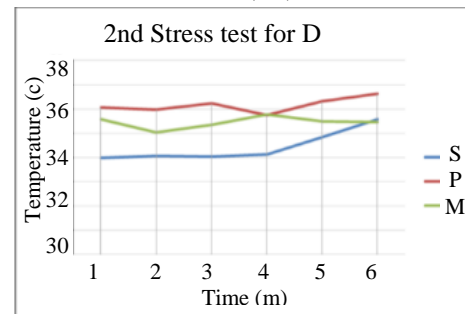
(C2)



(C1)



(D2)



(D1)

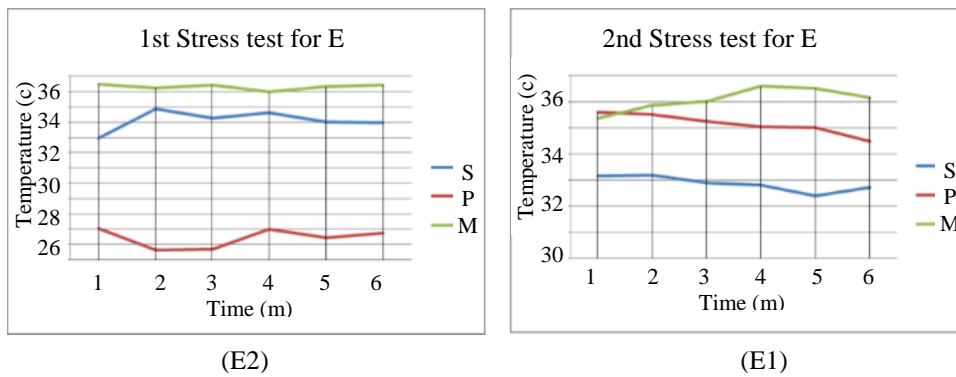


Figure 13: A(1)-E(1) Temperature of 5 subjects for the first time stimulus experiment conducted. A(2) - E(2) Temperature of 5 subjects for the second time stimulus experiment conducted. (average booth temperature :27.75 C, average booth humidity:43%)(Time (1): 1 minutes before stimulus , Time (2-5): Subsequent 1 minutes during stimulus, Time (6):1 minutes after stimulus)

In Figure 13 A(1)-E(1), 3 ROIs temperature differences are monitored for the first time. Subject is introduced with the stimulus test. Changes are detected mainly in the supraorbital areas. Out of 5 person, 2 person show visible blood vessel. Throughout the experiment, changes of temperature can be seen in the maxillary area. In Figure 13 A(2)-E(2), 3 ROIs temperature differences monitored for the 2nd time when subject is introduced with the stimulus test. Changes are also detected in the supraorbital areas where 2 out of 5 persons show visible blood vessel. Temperature changes can be seen in the maxillary area.

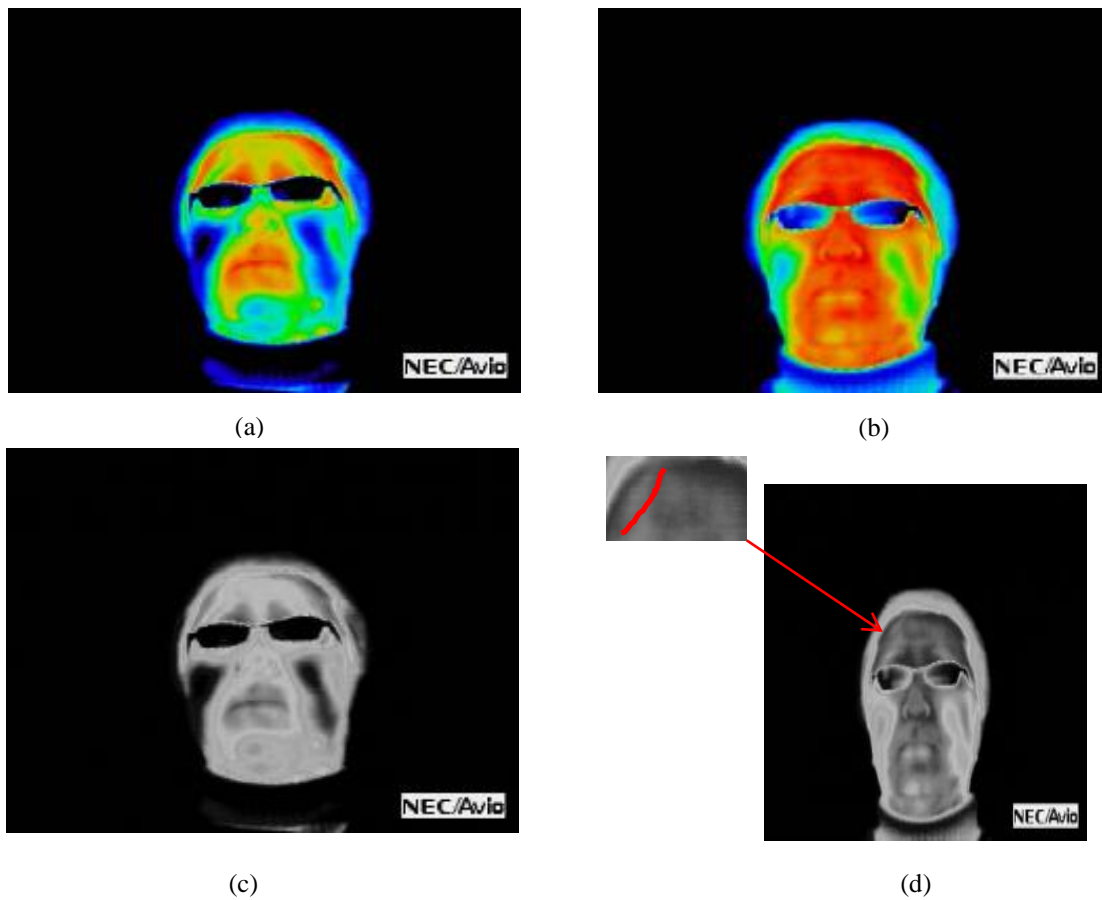


Figure 14: (a) Thermal (RGB)-before stimulus experiment (b)Thermal (RGB)-after stimulus experiment (c) Thermal (grayscale) Before stimulus experiment (d) (grayscale) after stimulus experiment-blood vessel visible

In the experiment conducted (Figure 14), several subjects show increased of heat especially at the supraorbital areas. It can be clearly seen by comparing the thermal (RGB) before and after stimulus experiment. Figure 14(c) is the grayscale of the thermal image before stimulus experiment whereby no blood vessel is visible. In Figure 14 (d) the blood vessel is visible.

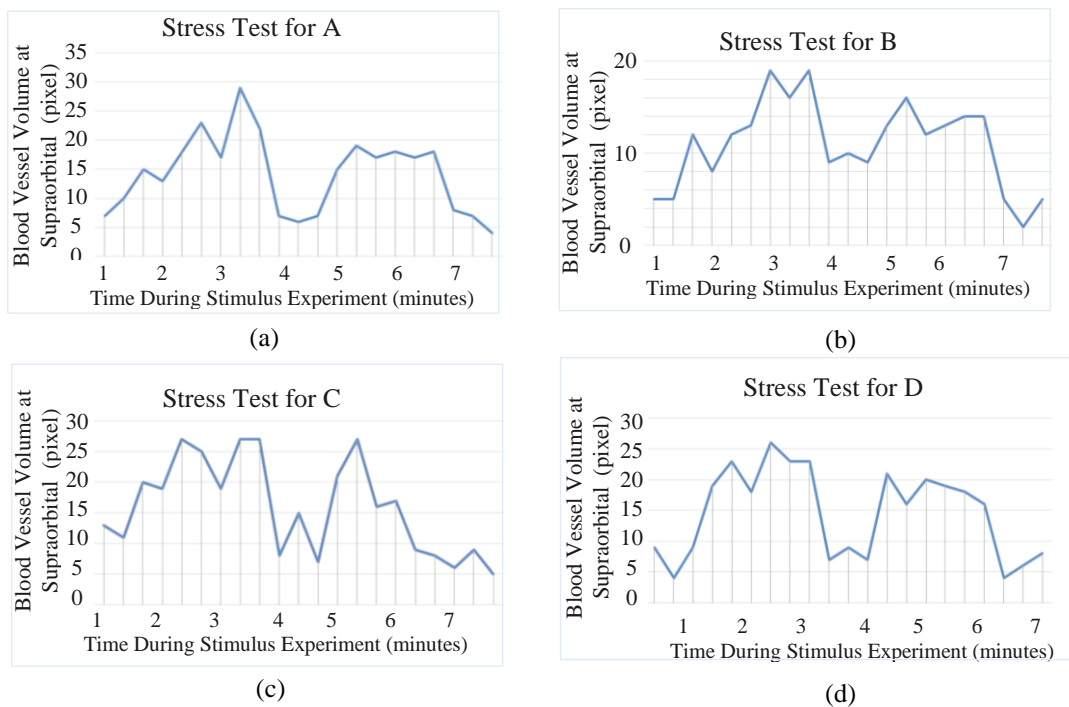


Figure 15: Blood Vessel Volume at Supraorbital for 4 correspondent %)(Time (1): 1 minutes before stimulus , Time (2-6): Subsequent 1 minutes during stimulus, Time (7):1 minutes after stimulus)

One of the most salient manifestation of sustained stress is that eyebrows frown more frequently [8]. The frowning is caused by contraction of the corrugator muscles. Activation of the corrugator muscles requires more blood, which is drawn from supraorbital vessel. Increase blood flow in supraorbital vessels, directly increases the cutaneous temperature on the forehead. As shown in figure 15. Therefore, mental stress is highly correlated with the activation of the corrugator muscle on the forehead.

4. DISCUSSION AND CONCLUSION

We have developed an Automatic Thermal Face, Supraorbital, Periorbital, Maxillary and Nostril Detection to be used for estimation of internal state. Several faces samples are taken in real time in our experimental setup to measure the effectiveness of our method . Almost 98% of correct measurement of ROI and temperature is detected. Feature matching experiment is also done to measure the effectiveness of our method of using nostril mask and shows positive results.

In the experiment which is monitoring the 3 ROIs temperatures before, during and after the stress stimulus, experiment was conducted 2 times. Thermal facial image also was monitored for possible blood vessel which is visible through the stress experiment. We have found out that user stress is correlated with the increased blood flow in three facial areas of sympathetic importance which is periorbital, supraorbital

and maxillary.

Mental stress is highly correlated with the activation of the corrugator muscle on the forehead. However segmenting the thermal imprints of the supraorbital vessels is challenging because they are fuzzy due to thermal diffusion and exhibit significant inter-individual and intra-individual variation. On the average the diameter of the blood vessels is 10-15 μ m, which is too small for accurate detection and 0.1 $^{\circ}$ C warmer than the adjacent skin.

Table 4: Feature Matching Between Nostril Mask (Thermal)- Visible Camera

	Chessboard	<i>FCP</i> Chessboard
Manufacturing	Printable from a standard printer	Printable from a standard printer with cheap fever cold plaster
Heating	A powerful (500W+) flood lamp and an external power supply are required. Difficult to get even coverage.	A powerful (500W+) flood lamp and an external power supply are required. Easy to get even coverage.
Footage	The pattern is only effective for a few seconds after heating.	The pattern can be used easily and effectively for about 15-20 minutes.
Searching	Generally requires preprocessing (inversion/ thresholding) Many conventional algorithms will struggle to find the pattern automatically	The algorithms are very common. No preprocessing required.
Accuracy	Less (<i>see experiment</i>)	Higher (<i>see experiment</i>)

In this paper, we are using a new approach in the registration of facial thermal-visible using nostril mask and by adopting SIFT feature point extraction and matching. Experiments show that this method shows 86% of correct matching. To further improve its accuracy, it requires more accurate samples and accurate Thermal-Visible camera calibration algorithm.

The comparison between traditional heated chessboard and *FCP* is shown in table 5. The cost involved in manufacturing *FCP Chessboard* is considered cheap in comparing to other calibration board made from polished copper plate coated with high emissivity paint or calibration rig. Even though heating is required in both method, it is difficult to get an even coverage comparing to our method. The pattern also can last longer about 20 minutes

ACKNOWLEDGMENT

This work was partially funded by the Japan Society for the promotion of Science (JSPS), Kagoshima University, Japan and University Tun Hussein Onn Malaysia (UTHM). We would like also to give special thanks to the Laboratory member for their invaluable inputs and assistance.

REFERENCES

- [1] Scheirer, J., Fernandez, R., Klein, J. and Picard, R. "Frustrating the user on Purpose: a step toward building an affective computer." *Interacting with Computers*, 14 (2002), 93-118.
- [2] Moulay Akhloufi, Abdelhakim Bendada, Jean Christophe Batsale, "State of the art in Infrared Face Recognition", *QIRT Journal*, Volume X, Pages 1-24.2008.
- [3] Mohd Norzali, Masayuki Kashima, Kiminori Sato, Mutsumi Watanabe "International Journal of Engineering Science and Innovative Technology (IJESIT)", December, 2012, Vol.1, Issue 2, pages 170-178, November 2012.
- [4] Mohd Norzali, Masayuki Kashima, Kiminori Sato, Mutsumi Watanabe "Thermal-Visual Facial Feature Extraction Based on Nostril Mask", *IAPR-Machine Vision Application 2013*, Kyoto, May 21-23, 2013.
- [5] J. Levine, I. Pavlidis, and M. Cooper, "The face of Fear", *Lancet*, vol. 357, no 9270, p.1757, Jun 2001.
- [6] I. Pavlidis, N.L. Eberhardt and J. Levine, "Human Behaviour: Seeing through the face of deception", *Nature*, vol. 415, no 6867, p.35, Jan. 2002.
- [7] Dvijesh, Manos Papadakis, P. Tsiamyrtzis, and I. Pavlidis, "Perinasal Imaging of Physiology Stress and Its Affective Potential" *IEEE Transactions on Affective Computing* Vol.3, No.3, July-September 2012.
- [8] Zhen Zu, Panagiotis Tsiamyrtziadis and Ionis Pavlidis, "The segmentation of the supraorbital vessels in thermal imagery" *IEEE fifth International Conferences in Advanced Video and signal based surveillance*, October 2008.
- [9] Z. Zhang, "A Flexible New Technique for camera calibration" *IEEE Trans. Pattern Anal. Mach. Intell.*, Vol.22, no. 11, pp. 1330-1334, Nov. 2000.
- [10] Hartley R. and Zisserman A., "Multiple view geometry in computer vision". *Cambridge University Press*, 2000.
- [11] Dvijesh A. Merla, P. Tsiamyrtzis, and I. Pavlidis, "Imaging Facial Signs of Neurophysiological Responses" *IEEE Transactions on Biomedical Engineering* Vo.56, No.2, February 2009.
- [12] J. Stemberger, R.S. Allison, T. Schell, "Thermal Imaging as way to classify Cognitive Workload", 2010 *Canadian Conference on Computer and Robot Vision*, pp.231- 283, 2010.

- [13] C.Puri, L.Eberhardt and J.Levine,"StressCam: Non-Contact measurement of users'emotional states through thermal imaging,"inProc. Of ACM Conf.Human Factors Computing System (CHI), 2-5, 2005, pp.1725-1728.
- [14] Jian-Gang Wang," Facial Feature Extraction in an Infrared Image by Proxy with a Visible Face Image"*IEEE Transc. On Instrumentations and Measurement, Vol 56, No 5*,pp 2057-2066,Oct. 2007.
- [15] Eberhard tan J.Levine," Human Behaviour: Seeing through the face of deception *Nature*, vol.415,no 6867,p.35,Jan.2002.
- [16] Dvijesh, Manos Papadakis, P. Tsiamyrtzis, and I. Pavlidis,"Perinasal Imaging of Physiology Stress and Its Affective Potential" *IEEE Transactions on Affective Computing Vol.3, No.3, July-September 2012*.
- [17] P.Ekmen, W.Friesen, and J. Hager, *The Facial Action Coding 2nd ed.* London: Weidenfeld & Nicolson (world), 2002.
- [18] Nandita Sharma, Tom Gedeon, Objective measures, sensors and computational techniques for stress recognition and classification: A survey, Australian Survey, Elsevier, *Computer methods and programs in Biomedicine 108(2012)*,1287-1301.